Mixed-Integer Real-time Control of a Building Energy Supply System

Artyom Burda[1,2], Dimitri Bitner[1], Felix Bestehorn[2], Christian Kirches[2], and Martin Grotjahn[1]

***Abstract*— We present a methodology based on mixed-integer nonlinear model predictive control for a real-time building energy management system in application to a single-family house with a combined heat and power (CHP) unit. The developed strategy successfully deals with the switching behavior of the system components as well as minimum admissible operating time constraints by use of a special switch-cost-aware rounding procedure. The quality of the presented solution is evaluated in comparison to the globally optimal dynamic programming method and conventional rule-based control strategy. Based on a real-world scenario, we show that our approach is more than real-time capable while maintaining high correspondence with the globally optimal solution. We achieve an average optimality gap of 2.5% compared to 20% for a conventional control approach, and are faster and more scalable than a dynamic programming approach.**

I. INTRODUCTION

Continuous development of energy supply and distribution systems by decentralisation of generation and storage, imposition of smart-homes technologies and dynamization of energy markets significantly complexifies the overall structural organization. The increasing complexity is particularly evident with respect to building energy supply components. In contemporary houses, diverse combinations of components such as gas boilers, combined heat and power units, storage units, solar/photovoltaic systems and many others exist. With the goal of energy efficiency and living comfort maximization, supervisory control of such systems with state-of-the-art methods for building energy management is particularly challenging. According to [1], where a highly comprehensive literature study on building energy consumption and intelligent automation systems was performed, potential savings of up to 30% can be achieved globally.

An intelligent real-time supervisory control system based on a model predictive control (MPC) strategy is getting more widespread. It can be considered as a promising candidate to exploit potential savings [1] and to replace conventional building control approaches eventually. In particular, a special case of MPC, nonlinear MPC (NMPC), is suitable for the control of nonlinear multidimensional systems. It is capable of explicitly operating with the system's nonlinear dynamics, objectives and constraints on control and state variables. It has already been used in various studies with different building energy system components and configurations, e.g in [2], where an NMPC-based controller showed a potential increase in the specific cooling power by 31.1% for absorption chillers, or [3], where the application to domestic micro-grid results in energy savings in the magnitude of 10%. A predictive controller was implemented as a real building temperature management system in [4] and achieved more than 17% savings compared to the conventional control.

In this paper, we present a special setup of a supervisory control strategy for a residential building energy system with a combined heat and power plant, based on mixed-integer nonlinear model predictive control (MI-NMPC). We take into account the system switching characteristics and along with continuously modulating operating range of the components, its minimum admissible operating times, so-called dwell-times. A procedure to tackle dwell-times restriction within the solar-driven climate system can be found in [5]. It also combines the means of MI-NMPC with a rather costly binary approximation problems solver *pycombina* [6]. Whilst in our case, we utilize a sophisticated and rapid rounding procedure presented in the section III-A.

We show that our strategy is able to handle the resulting optimization task of energy cost minimization while maintaining user comfort under the specified system constraints. We prove the performance of the suggested approach by comparison to a computationally very expensive but globally optimal solution obtained by dynamic programming. We evaluate the quality of the sub-optimal solution obtained by our approach in a comprehensive closed-loop simulation.

The article is structured as follows. First, we describe the considered building energy system and the resulting optimal control problem (OCP). Next, we present the solution approach with general formulations of the mixed-integer optimal control problem (MIOCP) and details on the rounding strategy. After that, the additionally required post-processing algorithm is described. Lastly, the numerical results illustrate the outcome of the proposed strategy in comparison to a dynamic programming method. Conclusions and an outlook on future work close the article.

II. OVERALL PROBLEM CLASS

A. System Description

The energy supply system considered here corresponds to the system from the authors' work [7]. Thereby, we provide only the information needed for the subject understanding and point out the characteristics not taken into account previously in the system model.

The energy supply system configuration is common for the residential sector (Fig. 1). It consists of a gas-driven modulating micro-CHP (combined heat and power) unit,

[1]Institute of Engineering Design, Mechatronics and Electromobility (IKME), Hannover University of Applied Sciences and Arts, Hannover, Germany {dimitri.bitner|artyom.burda|martin.grotjahn}@hs-hannover.de

[2]Institute for Mathematical Optimization, Technische Universität Carolo-Wilhelmina zu Braunschweig, Germany. {c.kirches|f.bestehorn}@tu-bs.de

 DOI: 10.1109/LCSYS.2022.3229159

which covers most of the energy demand of the building, a condensing boiler and a heat storage tank. The storage tank collects the generated thermal energy, which is then available for heating as well as for the demand-oriented hot water supply. The electricity generated by the CHP unit is consumed in the house itself. Surplus electricity can be fed into the public grid.

The optimal operation of the energy system central unit, CHP, appears to be rather challenging. Simultaneous generation of thermal and electrical energy must be taken into account along with the currently available storage capacity. An additional prediction of future heat consumption makes it possible to shift CHP operation times as well as electricity purchases and sales depending on the comfort requirements of the users and energy prices.

Another essential property not considered in previous work is the minimum operating time of CHP units, which is typically imposed by the manufacturer for durability reasons. For the current configuration, 60 minutes dwell time restriction is recommended by the maintenance instructions [8].

All the aforementioned system features lead to an economic optimal control problem with multiple objectives.

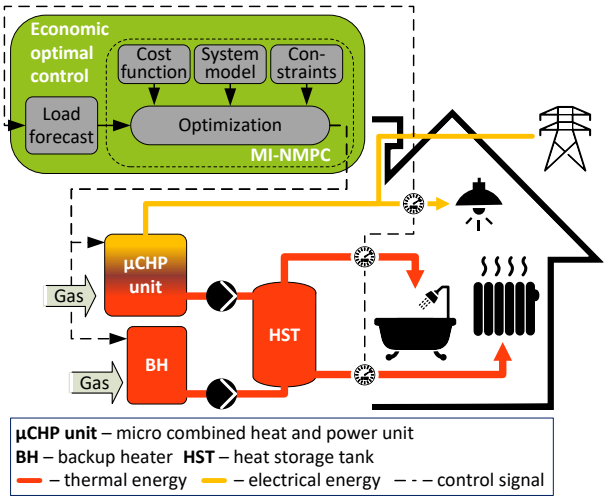

Fig. 1. The residential building energy system

B. System Model

The system model follows the one we presented in [7]. As understanding the main physical effects within the energy supply system is essential in the context of this work, we briefly present it here. We denote electrical power by P, thermal power by $\mathring{Q}$, input power of the CHP and boiler units by $\boldsymbol{u}^T = (u_{\mathrm{chp}}, u_{\mathrm{boi}})$, and introduce a binary control vector $\boldsymbol{v}^T = (v_{\mathrm{chp}}, v_{\mathrm{boi}})$ to represent the CHP and boiler on/off states. Description of the model parameters $a_{0,1,2}, b_{0,1,2}, A, c_{\mathrm{w}}, d_{0,1,2,3}, H_{\mathrm{fil,sto}}, m$ and $\Delta T_{\mathrm{chp,boi}}$ can be found in [7] with the corresponding values.

Electrical power generated by the CHP unit reads

$$P_{\mathrm{chp}}(t) = u_{\mathrm{chp}}(t) v_{\mathrm{chp}}(t). \tag{1}$$

It can be modulated continuously in the range $u_{\mathrm{chp}} \in [1.65, 4.55]$ (kW) when switched on ($v_{\mathrm{chp}} = 1$) and is zero when switched off ($v_{\mathrm{chp}} = 0$). Gas power $\mathring{Q}_{\mathrm{g,chp}}$ consumed when operating is calculated from the electrical energy efficiency characteristics η_{e} of the CHP unit by

$$\mathring{Q}_{\mathrm{g,chp}}(t) = \frac{P_{\mathrm{chp}}(t)}{\eta_{\mathrm{e}}(P_{\mathrm{chp}}(t))} = \frac{P_{\mathrm{chp}}(t)}{a_0 + a_1 P_{\mathrm{chp}}^2(t) + a_2 P_{\mathrm{chp}}(t)}, \tag{2}$$

where electric self-consumption of the CHP unit during operation is already taken into account. Thermal power is then derived from (2) and the thermal energy efficiency curve $\eta_{\mathrm{q}}(P_{\mathrm{chp}}(t)) = b_0 + b_1 P_{\mathrm{chp}}^2(t) + b_2 P_{\mathrm{chp}}(t)$. Thus, a quadratic relationship for the efficiency curves is assumed according to [9]. Thermal losses are assumed to be proportional to the temperature difference ΔT_{chp} to the ambient. This results in

$$\mathring{Q}_{\mathrm{chp}}(t) = \frac{P_{\mathrm{chp}}(t)\eta_{\mathrm{q}}(P_{\mathrm{chp}}(t))}{\eta_{\mathrm{e}}(P_{\mathrm{chp}}(t))} - H_{\mathrm{fil}} \Delta T_{\mathrm{chp}} v_{\mathrm{chp}}(t). \tag{3}$$

Similarly, the heating power of the gas-condensing boiler is

$$\mathring{Q}_{\mathrm{g,boi}}(t) = u_{\mathrm{boi}}(t) v_{\mathrm{boi}}(t) \tag{4}$$

with the modulated input power $u_{\mathrm{boi}} \in [6, 32]$ (kW). The thermal output power $\mathring{Q}_{\mathrm{boi}}$ is determined from the linear efficiency characteristics

$$\mathring{Q}_{\mathrm{boi}}(t) = d_2 \mathring{Q}_{\mathrm{g,boi}}^2(t) + d_3 \mathring{Q}_{\mathrm{g,boi}}(t) - H_{\mathrm{fil}} \Delta T_{\mathrm{boi}} v_{\mathrm{boi}}(t), \tag{5}$$

where, analogous to the CHP unit, thermal losses to the environment during the generation and distribution processes are also considered. In addition to gas, the condensing boiler also consumes a small amount of electrical power P_{boi} during operation. This is accounted for by the linear relationship

$$P_{\mathrm{boi}}(t) = d_1 \mathring{Q}_{\mathrm{g,boi}}(t) + d_0 v_{\mathrm{boi}}(t). \tag{6}$$

The dynamics of the buffer storage tank is modelled by simple energy balance ODE with $\mathring{Q}_{\mathrm{con}}$ as the building power demand, and ambient losses

$$\dot{Q}_{\mathrm{sto}}(t) = \mathring{Q}_{\mathrm{chp}}(t) + \mathring{Q}_{\mathrm{boi}}(t) - \mathring{Q}_{\mathrm{con}}(t) - H_{\mathrm{sto}} \tfrac{A}{m c_{\mathrm{w}}} Q_{\mathrm{sto}}(t). \tag{7}$$

Since we do not explicitly consider the actual volume flows and their temperatures, effects such as convection and conduction are omitted. Also, such effects as heating and cooling of the components can be neglected due to the large sampling time selected for the controller.

The energy sinks within the overall system consisting of the thermal $\mathring{Q}_{\mathrm{con}}$ and electrical P_{con} energy consumption in the building. From the controller's point of view, both are time-varying model parameters. The corresponding data is provided by measurements (in the current scenario these quantities are treated as system disturbances) or, when the model is deployed within a predictive controller, derived from an external energy demand forecast model.

C. System Control Problem

The overall goal of an energy supply system is a rather straightforward minimization of the overall energy expenses while ensuring supply of the required energy. To do so, we introduce auxiliary control variables $u_{\mathrm{el,buy}}$, $u_{\mathrm{el,sell}}$ for electricity purchases and sales and strive to satisfy the energy balance

$$(P_{\mathrm{con}}(t) + P_{\mathrm{boi}}(t) - P_{\mathrm{chp}}(t)) - u_{\mathrm{el,buy}}(t) + u_{\mathrm{el,sell}}(t) = 0. \tag{8}$$

Whenever the electricity demand is higher than the production, it is optimal to set the variable $u_{\text{el,buy}}(t)$ to the missing amount. A surplus electrical power situation is handled in just the opposite way using $u_{\text{el,sell}}(t)$. To obtain this behavior, the total expense consists of the costs for gas consumption at price c_1, costs for electrical power purchases from the grid at price c_3 offset by remunerations c_4 for self-generated electricity, and payments for feeding surplus electrical power into the grid at price c_2. This results in the Lagrange-type objective term

$$\begin{aligned} L(t,\boldsymbol{u}(t),\boldsymbol{v}(t)) = (\mathring{Q}_{\text{g,chp}}(t) + \mathring{Q}_{\text{g,boi}}(t))c_1 \\ - P_{\text{chp}}(t)c_4 + u_{\text{el,buy}}(t)c_3 - u_{\text{el,sell}}(t)c_2. \end{aligned} \tag{9}$$

The resulting system control problem is a mixed-integer optimal control problem (MIOCP), cf. [10], and reads

$$\min_{\boldsymbol{u}(\cdot),\boldsymbol{v}(\cdot)} \int_{t_0}^{t_\text{f}} L(\boldsymbol{u}(t),\boldsymbol{v}(t))\,\mathrm{d}t \tag{10a}$$
$$\text{s.t. } \dot{\boldsymbol{x}}(t) = f(\boldsymbol{x}(t),\boldsymbol{u}(t),\boldsymbol{v}(t)),\ t\in[t_0,t_\text{f}] \tag{10b}$$
$$\boldsymbol{x}(t_0) = \hat{\boldsymbol{x}}_0, \tag{10c}$$
$$\boldsymbol{x}(t) \in [\boldsymbol{x}_{\min},\boldsymbol{x}_{\max}], \quad t\in[t_0,t_\text{f}] \tag{10d}$$
$$\boldsymbol{u}(t) \in [\boldsymbol{u}_{\min},\boldsymbol{u}_{\max}], \quad t\in[t_0,t_\text{f}] \tag{10e}$$
$$\boldsymbol{0} \le \boldsymbol{c}(\boldsymbol{x}(t),\boldsymbol{u}(t),\boldsymbol{v}(t)),\ t\in[t_0,t_\text{f}] \tag{10f}$$
$$\boldsymbol{v}(t) \in \{0,1\}^2, \quad t\in[t_0,t_\text{f}] \tag{10g}$$

where $\boldsymbol{x} = (Q_{\text{sto}})$ represents the system state corresponding to the thermal energy stored in the tank, $\boldsymbol{u}^T = (u_{\text{chp}}, u_{\text{boi}}, u_{\text{el,buy}}, u_{\text{el,sell}})$ and $\boldsymbol{v}^T = (v_{\text{chp}}, v_{\text{boi}})$ denote the vectors of continuous and binary control functions. Constraint (10b) represents the system dynamics with (10d), (10e) as the state and input bounds and (10f) as the balance constraint.

III. Solution Approach

The system control problem (10) is a typical MIOCP instance. Binary control functions $\boldsymbol{v}$ enter nonlinearly and in a non-convex way in Eqs. (2, 3, 5). Hence, the problem is an NP-hard non-convex MINLP, cf. [11], after discretization in time. Moreover, it also is not immediately amenable to relaxation of the binary constraint, as the lower bound provided by such a relaxation could be arbitrarily bad [10]. Therefore, we make use of a partial outer convexification approach according to [10]. We introduce the one-hot encoding $\boldsymbol{\omega}(t) : \mathbb{S}^4 \to \Omega := \{0,1\}^2$ defined by

$$\boldsymbol{\omega}(t) \mapsto \boldsymbol{v}(t) = \textstyle\sum_{i=1}^4 \omega_i(t)\cdot v^i, \qquad t\in[t_0,t_\text{f}], \tag{11a}$$
$$\phi(\cdot,\boldsymbol{v}(t)) = \textstyle\sum_{i=1}^4 \omega_i(t)\cdot\phi(\cdot,v^i),\ \ t\in[t_0,t_\text{f}] \tag{11b}$$

where the set $\mathbb{S}^4$ lists the extremals of the 4-simplex excluding the origin, $v^i \in \Omega = \{0,1\}^2 = \{(0,0),(0,1),(1,0),(1,1)\}$ encodes the choices for $\boldsymbol{v}$, and ϕ is some arbitrary function of $\boldsymbol{v}$. Applying this to (10) results in an MIOCP that is linear and convex in the indicator function $\boldsymbol{\omega}$ point-wise in time. A relaxation is then obtained by replacing $\boldsymbol{\omega} \in \{0,1\}^4$ with $\boldsymbol{\alpha} \in [0,1]^4$. The resulting problem is a continuous OCP:

$$\min_{\boldsymbol{x},\boldsymbol{u},\boldsymbol{\alpha}} \int_{t_0}^{t_\text{f}} L_0(\boldsymbol{x}(t),\boldsymbol{u}(t)) + \sum_{i\in\Omega}\alpha_i(t)\cdot L_i(\boldsymbol{x}(t),\boldsymbol{u}(t))\,\mathrm{d}t \tag{12a}$$
$$\text{s.t. } \dot{\boldsymbol{x}}(t) = \boldsymbol{f}_0(\boldsymbol{x}(t),\boldsymbol{u}(t)) + \sum_{i\in\Omega}\alpha_i(t)\boldsymbol{f}_i(\boldsymbol{x}(t),\boldsymbol{u}(t)), \quad t\in[t_0,t_\text{f}], \tag{12b}$$
$$\boldsymbol{x}(t_0) = \hat{\boldsymbol{x}}_0, \tag{12c}$$
$$0 \le \boldsymbol{c}(\boldsymbol{x}(t),\boldsymbol{u}(t),\alpha(t)), \quad t\in[t_0,t_\text{f}], \tag{12d}$$
$$\boldsymbol{\alpha}(t) \in [0,1]^4,\ \textstyle\sum_{i=1}^4\alpha_i(t) = 1 \qquad t\in[t_0,t_\text{f}]. \tag{12e}$$

Herein, L_i, f_i and c_i denote evaluations of L, f, and c in (10) in mode $\boldsymbol{v}(t) = v^i \in \Omega$, while L_0 and f_0 are the mode-independent parts. One of the resulting relaxed indicator controls $\boldsymbol{\alpha}$ can be omitted since it can be directly calculated from the constraint (12e). Problem (12) can be solved using an established method for direct optimal control, e.g., direct multiple shooting [12] or direct collocation [13]. Let $(\boldsymbol{x}^N,\boldsymbol{u}^N,\boldsymbol{\alpha}^N)$ denote an optimal solution of a discretization of (12) on N elements in time. It is a property of formulation (12) shown in [14], that if a binary control $\boldsymbol{\omega}^N$ with

$$d(\boldsymbol{\omega}^N,\boldsymbol{\alpha}^N) := \max_{t\in[t_0,t_\text{f}]} \left\| \int_{t_0}^t \boldsymbol{\alpha}^N(s) - \boldsymbol{\omega}^N(s)\,\mathrm{d}s \right\|_\infty \le \varepsilon \tag{13}$$

can be found, then under Lipschitz assumptions one has

$$|\Phi(\boldsymbol{x}^N,\boldsymbol{u}^N,\boldsymbol{\alpha}^N) - \Phi(\boldsymbol{x}(\boldsymbol{u}^N,\boldsymbol{\omega}^N),\boldsymbol{u}^N,\boldsymbol{\omega}^N)| \le C\varepsilon.$$

for some constant C depending on bounds and Lipschitz constants. Herein, $\boldsymbol{x}(\boldsymbol{u}^N,\boldsymbol{\omega}^N)$ denotes the state trajectory obtained by solving (12b) using the binary control $\boldsymbol{\omega}^N$.

A. Switch-Cost Aware Rounding (SCARP)

In order to find such a binary control $\boldsymbol{\omega}^N$, [10] proposed a sum-up rounding (SUR) strategy with approximation bound $\varepsilon \in O(\log|\Omega|)$, cf. [14]. SUR controls come with high switching costs and have difficulties satisfying dwell time constraints, as observed in [15]. Since we have to ensure the durability of the CHP unit, it has a minimum operating time of $T_{\text{uptime}} = 60$ minutes when activated. We hence make use of a novel switch-cost minimizing reconstruction procedure first described in [16], [17]. To find $\boldsymbol{\omega}^N$, we solve the reconstruction problem

$$\min_{\boldsymbol{\omega}} \ \Gamma\left(\textstyle\sum_{i=1}^N \omega_i^N v^i\right) \ \text{s.t. } d(\boldsymbol{\omega}^N,\boldsymbol{\alpha}^N) \le \theta. \tag{14}$$

Herein, Γ is an objective function measuring a general switch cost term. In the present case, Γ penalizes violations of the CHP minimum uptime after every activation. The constraint on the approximation distance d defined in (13) ensures improving approximations as we choose finer grids. θ is a tuning factor that trades lower switch costs for better approximations of the relaxed optimal control. In the present case, it is set to $\theta = \overline{\mathscr{D}}(2|\Omega|-3)\overline{h}/(2|\Omega|-2)$, where $\overline{h}$ is the ratio of the largest non-equidistant interval to the smallest interval in the discretization and $\overline{\mathscr{D}}$ the largest dwell time constraint. For the examined problem this leads to $\theta = 25/3$ as $\overline{\mathscr{D}} = 10$, $|\Omega| = 4$ and $\overline{h} = 1$ as the grid is equidistant. This choice guarantees the existence of a binary control, see [18]. Computationally, problem (14) is solved using

the shortest-path approach of [17] with runtime complexity $O(N\sqrt{|\Omega|}2\theta+3)^{|\Omega|})$ [19], which is linear in N, the number of discretization points.

B. Post-processing

One of the main drawbacks of SCARP in practice is the lack of knowledge of the influence of rounding decisions on the system's state, and hence on path constraints. This can lead to constraint infeasibility when a binary control output is directly applied to the real system. In the performed simulation study, constant violation of the state constraints has been noticed at times of low thermal storage load. In order to prevent this from happening, we propose the following post-processing algorithm:

1) Set the number of future time steps for which the integer control must remain constant according to the dwell times count provided by SCARP to enforce the feasibility of all dwell time constraints;

2) Include an additional constraint to maintain the dwell times restriction $\sum_{k=1}^{N_d} \alpha_k - p_{\text{dwt}} \leq 1$, where N_d is the number of controls following a dwell time restriction and the parameter p_{dwt} is set to 1 to force $\alpha_k = 0$ during an active dwell time restriction;

3) For SCARP, all binary indicators after convexification that correspond to the active state of one of the initial integer controls are considered identical. For instance, we have two controls α_2 encoding $\boldsymbol{v} = (1,0)^T$ and α_3 encoding $\boldsymbol{v} = (1,1)^T$ that both encode an ON state of the CHP unit and therefore must be considered together when CHP dwell times are handled. We initialize the relaxed indicators with $\alpha_k = \frac{1}{N_d}$ (in our case, $\alpha_2 = \frac{1}{2}$; $\alpha_3 = \frac{1}{2}$) in order to satisfy (12e);

4) Solve the resulting relaxed continuous OCP;

5) In most cases, we observed integrality already after solving the relaxed continuous OCP, cf. [10] for an explanation based on the bang-bang principle. If, however, a fractional feedback control vector is obtained, the common rounding to the nearest integer procedure is performed for this control only, and the continuous optimization problem is solved again with fixed binary controls to find the corresponding continuous controls and the differential state. The remaining degrees of freedom in the continuous controls suffice to satisfy the path constraints if the box $[\boldsymbol{u}_{\min}, \boldsymbol{u}_{\max}]$ is sufficiently large and if $\partial c/\partial u(\cdot, \alpha(t))$ has full row rank. In absence of this regularity property, however, this final step is of heuristic nature.

Figure 2 illustrates the state trajectory resulting from this strategy for a time slice particularly difficult to handle. High

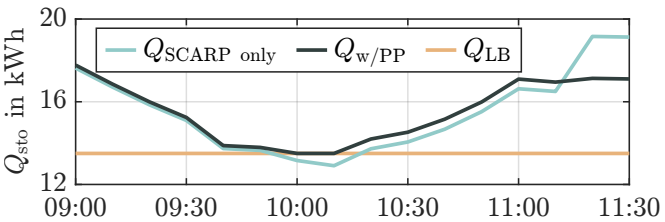

Fig. 2. State trajectories for different strategies. $Q_{\text{w/ PP/LB}}$ indicate the resulting trajectory with the presented post-processing algorithm (w/ PP) and the lower state bound (LB), respectively.

energy consumption leads the energy level in the storage to be drowned to its permitted minimum. Even if the violation of the constraint is only minor, the consequences of this violation can be rather serious in individual cases. As a decisive improvement, the proposed approach guarantees the compliance of the solution with all path and dwell time constraints.

IV. Results

A. Dynamic Programming

To evaluate the performance of the proposed control approach, we compare the approximate solution with the globally optimal one determined by dynamic programming (DP). To do so, OCPs are solved by means of the *dpm*-function from [20] in Matlab. For this purpose, the model and cost function described in equations (1-9) are discretized by an Euler forward approximation using a step-size of $T_{\text{S}} = 600$ s. The minimum operating time of the CHP unit is maintained via a counter c_{dwt} realized by an additional state variable and is set to zero after each shutdown of the CHP unit according to $c_{\text{dwt},k+1} = v_{\text{intm}}(v_{\text{intm}} c_{\text{intm}} + c_{\text{dwt},k})$, where

$$v_{\text{intm}} = \begin{cases} 1 & \text{if } 0 < c_{\text{dwt},k} < T_{\text{uptime}}/T_{\text{S}} \\ v_{\text{chp}} & \text{else} \end{cases} \tag{15}$$

and

$$c_{\text{intm}} = \begin{cases} 1 & \text{if } c_{\text{dwt},k} < T_{\text{uptime}}/T_{\text{S}} \\ 0 & \text{else} \end{cases} . \tag{16}$$

The distinction between feed-in and purchase of electrical power is modelled by means of sign-functions within the cost function. We have chosen the resolutions $\Delta u_{\text{chp}} = 150$ W, $\Delta v_{\text{chp}} = 1$, $\Delta Q_{\text{sto}} = 1014$ Wh and $\Delta c_{\text{dwt}} = 1$ to discretize the continuous input and state variables to obtain manageable *dpm* runtimes. The boiler and its control variables are neglected here, since backup heating is not needed during the particular period under consideration. However, for periods with higher thermal consumption the boiler must be taken into account, by which DP runtimes would become much slower. These settings result in a total number of $N = 21 \cdot 2 \cdot 37 \cdot 7 > 10^4$ discretization points to be evaluated per feedback iteration.

B. Simulation results

In order to achieve real-time behavior of the controller, the aforementioned model is implemented in the state-of-the-art numerical optimal control software package *acados* [21]. A direct multiple shooting algorithm is used for the discretization and parameterization of the OCP. The resulting nonlinear programming problem is solved by an early-terminated sequential quadratic programming (SQP) approach using the interior-point solver HPIPM [22] for the underlying quadratic programs (QP). Standard parameters of *acados* solver are used except for Hessian calculation, where the exact Hessian method with mirror [21] regularization strategy is applied.

The long-term simulation run of the system with the presented control approach is depicted in Figure 3. The simulation has been performed with a sampling time of

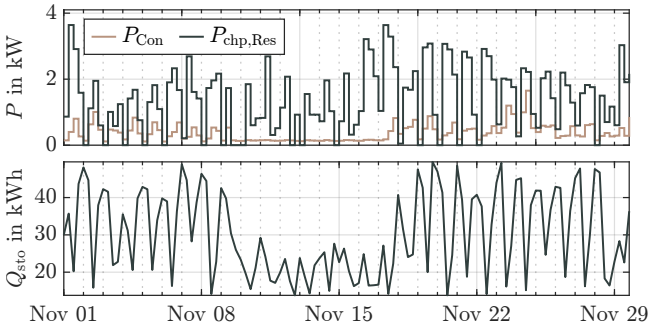

Fig. 3. Total electricity demand P_{Con}, production $P_{\text{chp,Res}}$ accumulated by 6 hours (top) and storage state Q_{sto} (bottom) for a one-month system simulation using the proposed strategy.

$T_{\text{S}} = 600\,\text{s}$ and a prediction horizon of 24 hours. We show total electricity demand and production with the thermal energy storage state aggregated by 6 hours. An important observation here is that the thermal energy generation is clearly shifted to the high electricity demand periods. Of course, this corresponds to the expected behavior, as the CHP electrical efficiency peaks with its high production value.

We compare the proposed solution with the globally optimal dynamic programming method described in the previous section. Evaluation takes place for different scenarios using energy data for one week from a single-family building. We additionally show the corresponding results for the state-of-the-art conventional rule-based control strategy (SoA). This heat-led strategy is based on the documentation in the CHP unit manufacturer's manual [8]. The CHP is modulated subject to the current production level (low, medium and high) and the storage state.

Table I shows the resulting cost differences and calculation times for 6 days. We provide calculation times needed for one-day closed-loop simulation, hence, for 144 simulation steps. The average feedback time is given in the table as well. It can be seen that the dynamic programming method is comparatively fast and is also real-time capable for the particular system. However, it must be taken into account that such a result was possible only due to the simplicity of the considered problem and resulting solution trajectory. For more sophisticated, more dimensional systems "curse of dimensionality" would lead to a strong increase in the computation time, which diminishes its practical applicability. Whereas the design of the presented algorithm ensures its scalability properties and therefore practical relevance even for relatively complex systems.

For one-day closed-loop simulation, an average optimality gap of 2.5% in the objective was achieved for the presented control strategy in contrast with 20% for the SoA approach. Continuous simulation for the whole week brings a 2.5% cost difference in comparison to the SoA with 18.9%.

TABLE I
COMPARISON OF RUNTIMES AND OBJECTIVE DIFFERENCE

Day	Calculation Time [s]				Objective Difference to DP	
	per Feedback		Total			
	NMPC	DP	NMPC	DP	NMPC	SoA
1	0.40	1.41	57.3	203.0	3.5%	13.0%
2	0.41	1.39	59.1	200.6	1.2%	25.4%
3	0.41	1.39	58.6	200.5	3.8%	29.6%
4	0.42	1.38	59.8	199.4	2.8%	11.5%
5	0.40	1.38	57.6	198.2	2.1%	19.3%
6	0.40	1.32	58.0	190.6	1.1%	20.2%
1-6	0.40	1.38	347.4	1192.3	2.5%	18.9%

As mentioned, the problem is solved by means of an early terminated SQP approach. While it would have been preferable to utilise an SQP real-time iterations (RTI) approach, the key challenge for the nonlinear solver here is the adaptation to the changing energy consumption data, which corresponds to rapidly nonlinear disturbances. A representative example is shown with P_{Con} in Figure 4. In our case, under the specified sampling times, an SQP RTI method was unable to quickly reject these disturbances and led to inferior objective function values. In order to tackle this problem, we increased the number of SQP iterations for the continuous problem at each time step. A value of 20 iterations was found to allow the solver to converge with correspondence to the incoming disturbance data and yielded satisfactory results. Larger values provided only diminishing extra returns. To cope with a poor initial trajectory guess that does not make use of scenario data, the number of SQP iterations is set to a higher value of 100 on the first time step only.

Obviously, the number of SQP iterations could be decreased based on the disturbance strength, i.e., it could be lowered at time steps where the disturbance does not

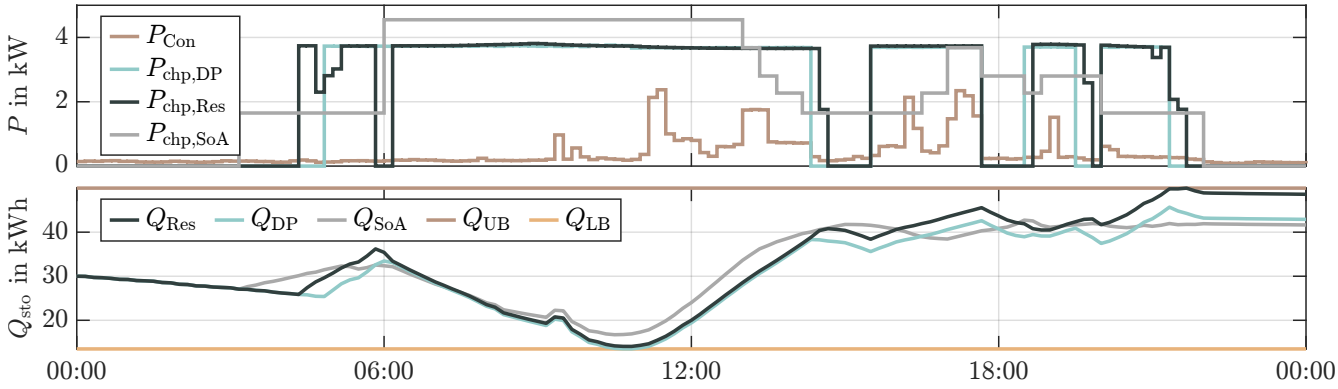

Fig. 4. Trajectories of the power supply system with electrical power demand from the customer P_{Con}, power P_{chp} generated by the CHP, and thermal energy state Q_{sto} of the storage. Results for DP and the proposed approach (Res) respectively. (UB) and (LB) are upper and lower state bounds.

exceed several percentage points of the maximum power output. A solution here might be a termination factor, which depends on the current KKT (Karush–Kuhn–Tucker) residual retrieved from the solver. When the desired KKT threshold has been reached, the solver proceeds with the next time step. This modification is subject to further work.

Figure 4 illustrates the resulting trajectories for the generated electrical power as well as the energy level in the storage. We omit the trajectories for the boiler power output, as its operation is uneconomical for the current period and all the control strategies follow this behavior. Apart from that, it can be seen that CHP unit operation trajectory tends to be bang-bang. Since there is a higher need for electrical energy and its production efficiency is maximum when the CHP is operating at full power (see the efficiency curve in [7]), this corresponds to the beforehand expected behavior. Deviations in the trajectories of the achieved solution from the globally optimal results, obviously, persist. Yet, the method, proposed in this paper, still shows high agreement with the globally optimal solution. For the presented period the total energy costs difference is 3.5% contrary to 13% for the SoA strategy. Furthermore, with a computational time of less than one minute for the simulation period of one whole day, the presented approach has proven to be real-time capable even on lean embedded hardware.

V. CONCLUSIONS

A novel approach for building energy supply systems supervisory control has been presented. It enables real-time operation management of sophisticated building energy systems without the need for additional technical modifications. Combining mixed-integer nonlinear optimal control methods with an advanced switch-cost-aware rounding approach, we were able to achieve notable performance results. We have shown that the presented strategy shows high agreement with the globally optimal solution in a closed-loop simulation. In comparison to dynamic programming, an average optimality gap of 2.5% in objective for the selected period was achieved while state-of-the-art control strategy shows an average 20% difference in cost. At the same time, we have taken into account the requirement for a minimum admissible operating time of the system components which is particularly common in building energy management. As a result, our approach makes it possible to exploit almost the entire cost and energy-saving potential of the system while ensuring real-time capability as an essential prerequisite for use in practice.

Future work consists of an investigation of the performance and stability properties of the presented algorithm as well as the practical implementation of the strategy in a real building. Application of the developed strategy to a more complex system of multifamily residential units is also a subject of further work.

ACKNOWLEDGMENT

TUBS discloses funding by DFG (Ki 1839/1-2, Ki 1839/3-1) and by BMBF (05M20MBA-LEOPLAN). IKME is partly financed by the BMWK (03EN1007A-EEBF).

REFERENCES

[1] P.H. Shaikh, N. Bin Mohd Nor, P. Nallagownden, I. Elamvazuthi, and T. Ibrahim. A review on optimized control systems for building energy and comfort management of smart sustainable buildings. *Renewable and Sustainable Energy Reviews*, 34:409–429, 2014.

[2] U. Bau, N. Baumgärtner, J. Seiler, F. Lanzerath, C. Kirches, and A. Bardow. Optimal operation of adsorption chillers: First implementation and experimental evaluation of a nonlinear model predictive control strategy. *Applied Thermal Engineering*, 149:1503–1521, 2019.

[3] G. Bruni, S. Cordiner, V. Mulone, V. Sinisi, and F. Spagnolo. Energy management in a domestic microgrid by means of model predictive controllers. *Energy*, 108:119–131, 2016. Sustainable Energy and Environmental Protection 2014.

[4] Samuel Privara, Jan Široký, Lukáš Ferkl, and Jiří Cigler. Model predictive control of a building heating system: The first experience. *Energy and Buildings*, 43:564–572, 01 2010.

[5] A. Bürger, D. Bull, P. Sawant, et al. Experimental operation of a solar-driven climate system with thermal energy storages using mixed-integer nonlinear model predictive control. *Optimal Control Applications and Methods*, 42, 05 2021.

[6] A. Bürger, C. Zeile, M. Hahn, A. Altmann-Dieses, S. Sager, and M. Diehl. pycombina: An open-source tool for solving combinatorial approximation problems arising in mixed-integer optimal control. *IFAC-PapersOnLine*, 53(2):6502–6508, 2020.

[7] D. Bitner, A. Burda, and M. Grotjahn. Optimized supervisory control of a combined heat and power plant by mixed-integer nonlinear model predictive control. `http://dx.doi.org/10.13140/RG.2.2.11938.50883`. In *NEIS 2021*. VDE Verlag, 2021.

[8] Vaillant GmbH. *Installations- und Wartungsanleitung mikro-BHKW ecoPOWER*, 2012.

[9] I. Beausoleil-Morrison and N. Kelly. Specifications for modelling fuel cell and combustion-based residential cogeneration device within whole-building simulation programs. *IEA/ECBCS Annex 42 Report*, 10 2007.

[10] S. Sager. *Numerical methods for mixed–integer optimal control problems*. Der andere Verlag, Tönning, Lübeck, Marburg, 2005.

[11] L. Liberti. Undecidability and hardness in mixed-integer nonlinear programming. *RAIRO - Operations Research*, 53(1):81–109, 2019.

[12] H.G. Bock and K.J. Plitt. A Multiple Shooting algorithm for direct solution of optimal control problems. In *Proceedings of the 9th IFAC World Congress*, pages 242–247, Budapest, 1984. Pergamon Press.

[13] L.T. Biegler. Solution of dynamic optimization problems by successive quadratic programming and orthogonal collocation. *Computers & Chemical Engineering*, 8:243–248, 1984.

[14] C. Kirches, F. Lenders, and P. Manns. Approximation properties and tight bounds for constrained mixed-integer optimal control. *SIAM J. Cont. Opt.*, 58(3):1371–1402, February 2020.

[15] A. Bürger, C. Zeile, A. Altmann-Dieses, S. Sager, and M. Diehl. Design, implementation and simulation of an MPC algorithm for switched nonlinear systems under combinatorial constraints. *Journal of Process Control*, 81:15–30, 2019.

[16] F. Bestehorn, C. Hansknecht, C. Kirches, and P. Manns. A switching cost aware rounding method for relaxations of mixed-integer optimal control problems. *Proceedings of the 58th IEEE Conference on Decision and Control (CDC 2019)*, pages 7134–7139, 12 2019.

[17] F. Bestehorn, C. Hansknecht, C. Kirches, and P. Manns. Mixed-integer optimal control problems with switching costs: A shortest path approach. *Mathematical Programming*, 188:621–652, 2021.

[18] C. Zeile, N. Robuschi, and S. Sager. Mixed-integer Optimal Control under Minimum Dwell Time Constraints. *Math. Prog.*, pages 1–42, 2020.

[19] Felix Bestehorn. *Combinatorial algorithms and complexity of rounding problems arising in Mixed-Integer Optimal Control*. PhD thesis, Technische Universität Carolo-Wilhelmina zu Braunschweig, 2022.

[20] O. Sundstrom and L. Guzzella. A generic dynamic programming Matlab function. In *2009 IEEE International Conference on Control Applications*, pages 1625–1630. IEEE, 08.07.2009 - 10.07.2009.

[21] R. Verschueren, G. Frison, D. Kouzoupis, J. Frey, N. van Duijkeren, A. Zanelli, B. Novoselnik, T. Albin, R. Quirynen, and M. Diehl. acados – a modular open-source framework for fast embedded optimal control. *Mathematical Programming Computation*, Oct 2021.

[22] G. Frison and M. Diehl. HPIPM: a high-performance quadratic programming framework for model predictive control, 2020.